



Response surface methodology approach for optimization of color removal and COD reduction of methylene blue using microwave-induced NaOH activated carbon from biomass waste

Ali H. Jawad^{a,*}, Mohd Azlan Mohd Ishak^b, Ahlam M. Farhan^c, Khudzir Ismail^a

^aCoal and Biomass Energy Research Group, Faculty of Applied Sciences, Universiti Teknologi MARA, 40450 Shah Alam, Selangor, Malaysia, Tel. (+603) 55211721; emails: ahjm72@gmail.com, ali288@salam.uitm.edu.my (A.H. Jawad); Tel. (+603) 55444562; email: khudzir@salam.uitm.edu.my (K. Ismail)

^bCoal and Biomass Energy Research Group, Faculty of Applied Sciences, Universiti Teknologi MARA, 02600 Arau, Perlis, Malaysia, Tel. (+604) 9882027; email: azlanishak@perlis.uitm.edu.my

^cChemistry Department, College of Sciences for Women, Baghdad University, Iraq, Tel. (+964) 7702507225; email: ahlam63a@yahoo.com

Received 26 March 2016; Accepted 31 July 2016

ABSTRACT

Coconut leaves (*Cocos nucifera*. L) biomass waste were utilized for the preparation of activated carbon by microwave-induced NaOH activation. The surface characteristics of the coconut leaves activated carbon (CLs-AC) were determined by scanning electron microscopy, Fourier transform infrared spectroscopy and pH_{PZC} . Subsequently, the CLs-AC was applied for the color removal and chemical oxygen demand (COD) reduction of methylene blue (MB) from aqueous solutions. The face-centered composite design (FCCD) and response surface methodology were used to investigate the effects of main operating variables such as initial solution pH (3–8), temperature (298–323 K), adsorbent dosage (0.2–1.50 g/L), and contact time (15–90 min), while the initial MB concentration was fixed at 100 mg/L throughout the optimization process. Maximum color removal (99.37%) and COD reduction (98.27%) for MB can be achieved by simultaneous interaction between temperature with time and adsorbent dosage with contact time. The optimum pH, temperature, adsorbent dosage and contact time were found to be 8.00, 323.00 K, 1.50 g/L and 90 min, respectively. Under optimal conditions, the adsorption equilibrium data was well fitted with the Langmuir adsorption isotherm with R^2 of 0.9907 and q_{max} at 87.72 mg/g. The adsorption kinetics was found to follow pseudo-second-order model.

Keywords: Optimization; Response surface methodology; Decolorization; Chemical oxygen demand; Adsorption; Activated carbon

1. Introduction

Color effluents in wastewaters are sourced from the use of dyes and pigments in the printing, textiles, paper, carpet, leather, rubber, plastic, cosmetics, food and pharmaceutical industries [1]. The increased use of synthetic dyes in process industries has become a serious environmental problem. Color in wastewater has become well-known environmental problem and direct destruction to the aquatic system, because dyes are considered as hazardous, toxic, not biodegradable, and

tend to suppress photosynthetic activity in aquatic system by preventing the penetration of sunlight and oxygen, high level of the chemical oxygen demand (COD) and total organic carbon (TOC) [2]. The highest rates of toxicity were recognized among basic and diazo direct dyes [3]. Furthermore, most of these dyes have direct and indirect toxic effects on humans as they can cause allergy, dermatitis, cancer, jaundice, tumors, skin irritation, allergies, heart defects and mutations [4].

Basic dyes are cationic dyes with cationic characteristics originating from positively charged nitrogen or sulfur atoms in dye molecular structure. They present an obvious coloration even at concentration less than 1 mg/L. Basic dyes have

* Corresponding author.

been classified as toxic colorants [5]. Methylene blue (MB) is the most important basic dye. It has been widely used in industrial activities such as dyeing, dyeing leather, printing calico, printing cotton and tannin, in addition to some other biological uses [6]. The acute exposure to MB dye can cause eye burns, and if swallowed, it causes irritation to the gastrointestinal tract with symptoms of nausea, vomiting and diarrhea [7]. MB dye may also possibly cause methemoglobinemia, cyanosis, convulsions and dyspnea if inhaled [8].

Among various treatment methods have been applied in water treatment technologies such as bioremediation [9], electrochemical degradation [10], cation exchange membranes [11], Fenton chemical oxidation [12] and photocatalysis [13–15]. Adsorption is one of the most effective processes for the removal of organic and inorganic pollutants from water even at concentrations as low as 1 mg/L [16]. Many non-conventional adsorbents have been utilized for water remediation, including inorganic adsorbents, organic adsorbents and biomass. Activated carbon (AC) has been proven to be superior material for water and wastewater treatment due to its high surface area, well-developed pore structure, capability for efficient adsorption of a broad range of adsorbates and its simplicity of design [17].

However, the high cost of the commercially available ACs limits their use as an adsorbent. In recent years, much research on water decontamination has focused on the identification of renewable and cheaper precursors for preparation of ACs and methods for their modification by chemical and physical activation [18–23]. In these activation methods, heat is transferred to the samples by conduction and convection mechanisms. The surface of the ACs is heated before their interiors. This thermal gradient leads an inhomogeneous microstructure for high heating rates [24]. As an alternative heating method, microwave irradiation has introduced promising results over the last several years in the production of AC. By using microwave technique, it is possible to produce AC by a convenient and a quick way. Microwaves supply energy to the carbon particles, and this energy is converted into heat within the particles themselves by dipole rotation and ionic conduction. Microwave heating has the advantages of rapid temperature rise, uniform temperature distribution and saving of energy over conventional heating method [25].

Malaysia is the tenth largest producer of coconut (*Cocos nucifera* L.) in the world, which generates a large amount of waste from this fruit. Coconut leaves is one of the lignocellulosic materials of solid biomass wastes with no economic impact and often bring about serious disposal problem to the surrounding environments [26]. The use of the coconut leaves as a precursor for the production of AC by microwave-assisted NaOH activation, so far, has not been reported in the literature yet. The use of alkaline metal such as KOH and NaOH as activating agents has been found efficient in AC preparation with well-developed porosity, a narrow pore size distribution and high surface area [27–35]. Tseng [36] reported that NaOH activation has several advantages compared with KOH activation such as: (i) cheaper, (ii) lower percentage of activator, (iii) more eco-friendly, and (iv) less corrosive.

Therefore, the key objectives of this study were to develop a low-cost AC adsorbent developed from coconut leaves by using microwave heating technique in the presence

of an environmental friendly chemical activator like NaOH. Furthermore, to test the effectiveness of the received AC for the color removal and COD reduction of MB from the aqueous solution by optimizing the adsorption conditions with assist of the statistical software of the response surface methodology (RSM). The effect of the crucial factors, including initial solution pH, temperature, adsorbent dosage, and contact time on color removal and COD reduction of MB was investigated. The face-centered composite design (FCCD) and RSM were used to investigate the effects of major operating variables and optimization conditions on the color removal and COD reduction. After determining the optimal adsorption conditions, the removal capacity of CLs-AC adsorbent was established by applying different models of isotherms and adsorption kinetics. Recent works have proved that RSM could serve as a powerful statistical tool for optimization of the process parameters [37–39].

2. Materials and methods

2.1. MB aqueous solution

The basic dye, MB (CI 52015, chemical formula = $C_{16}H_{18}ClN_3S \cdot xH_2O$, molecular weight of 319.86 g/mol, nature = basic blue, $\lambda_{max} = 661$ nm) was obtained from R&M Chemicals, Malaysia. Stock MB solution, 1,000 mg/L was prepared by dissolving 1 g of MB in ultrapure water ($18.2 \text{ M}\Omega \text{ cm}^{-1}$) until the solution reaches 1 L. The stock solution was then kept in a dark condition at room temperature prior to use.

2.2. Preparation of AC

The fallen coconut leaves (CLs) waste biomass was obtained from Universiti Teknologi MARA, Arau Campus, Perlis, Malaysia. The sample was washed thoroughly using tap water to remove any impurities prior to drying in an oven (Memmert, model UFB-400) at 80°C for 48 h. The dried sample was then cut into smaller pieces before grinding to powder form ($150\text{--}212 \mu\text{m}$). The coconut leaves activated carbon (CLs-AC) was prepared by mixing predetermined 10 g of CLs powder with 40 mL of 50% (w/v) NaOH solution at impregnation ratio of (1:4 w/v). The sample was next placed inside an oven at 110°C for 24 h until completely dried. The dried sample was activated by using a quartz glass reactor (7.5 cm diameter and 8.5 cm length). The reactor was sealed at bottom and open from the top end to allow for the escape of the pyrolysis gases. The carbonization process was conducted under high purified nitrogen gas (99.99%) as an inert gas. Pyrolysis of sample was carried out in a modified microwave heating oven, model Panasonic NNJ-993 with at fixed power of 600 W for 20 min at frequency of 2,450 MHz. The schematic diagram of the microwave-assisted pyrolysis system was exactly as described in previous work [40]. After cooling, the resulting mixture was washed with 0.1 M solution of HCl followed by hot distilled water until pH ~ 6.5 to eliminate activating agent residues and other inorganic species formed during the process. After that, the final AC developed from coconut leaves (CLs-AC) sample was dried at 110°C for 24 h, and then weighed to determine the yield of the CLs-AC product. The CLs-AC was ground, and the

powder sieved to obtain a particle size range of 150–212 μm of CLs-AC powder. Finally, the CLs-AC was stored in tightly closed bottles.

2.3. Characterization of CLs-AC

The yield of CLs-AC was calculated based on the published method [41]. The percentage yield of the CAC was calculated by using Eq. (1):

$$\text{Yield (\%)} = \frac{\text{Wt. of CAC}}{\text{Wt. of dried coconut leaves}} \times 100 \quad (1)$$

The iodine number, which is a measure of the micropore content of AC (0–20 \AA), was determined according to the standard method [42]. The bulk or apparent density was determined following the reported method [43]. The moisture content was determined using oven drying method [44]. The ash content was determined by standard methods [45]. The point of zero charge (pH_{pzc}) of CLs-AC was determined using a series of closed vessels containing 50 mL of 0.1 N KNO_3 solutions. The initial pH (pH_i) of solution was adjusted between 2 and 12 using 0.1 M HCl or NaOH solution. Approximately 1 g of CLs-AC was added to each flask containing different pH of solution. These flasks were agitated for 24 h at atmospheric conditions. The final pH (pH_f) was measured for each flask. The obtained results were plotted as ($\text{pH}_i - \text{pH}_f$) vs. pH_i . The point at which the curve crossed the line $\text{pH}_i = \text{pH}_f$ was determined as pH_{pzc} [46]. The surface morphology of CLs-AC before and after adsorption of MB was examined using scanning electron microscopy (SEM-EDX, FESEM CARL ZEISS, SUPKA 40 VP). The functional groups of CLs-AC before and after MB adsorption were detected by Fourier transform infrared (FTIR) spectroscope (PerkinElmer, Spectrum RX I). The spectra were recorded from 4,000 to 400 cm^{-1} .

2.4. Experimental methods and measurement

Based on the preliminary tests, the experiments were carried out under various operating conditions such as initial solution pH (3–8), temperature (298–323 K), adsorbent dosage (0.2–1.5 g/L), and agitation time (15–90 min), while the initial MB concentration was fixed at 100 mg/L throughout the optimization process. Another operating factor with least effect such as shaking speed was excluded from the optimization process. For each run, 0.1 L of the dye solution with an initial dye concentration of 100 mg/L with desired pH was introduced into a 0.25-L Erlenmeyer flask, which contained a certain amount of adsorbent. The flask was then placed in the water bath shaker (Mettler, waterbath, model WNB7-45, Germany) at a certain temperature and fixed shaking speed of 90 strokes/min. After a desired contact time, the flask was withdrawn from the shaker. COD test was performed according to the analytical procedure [47] by using COD reactor (DRB 200, HACH, USA). The color and COD removal were determined by using a direct reading spectrophotometer (DR 2800 HACH, USA) at λ_{max} 661 and 620 nm, respectively. The pH was adjusted to a desirable value using 0.1 M NaOH or HCl using a pH meter model 827 (Metrohm Herisau,

Switzerland). Each experiment was repeated three times. In order to account for color leached by the adsorbent and adsorbed by the glass containers, blank runs with only the adsorbents in 0.1 L of doubly distilled water and 0.1 L of dye solution without any adsorbent following the analytical method described by Hameed et al. [48]. Moreover, adsorption experiments were conducted in triplicate under identical conditions and the results are reported as an average value.

The percentage of MB color removal in the aqueous solutions by CLs-AC was calculated by the following equation:

$$\text{Color removal (\%)} = \left(\frac{C_0 - C_t}{C_0} \right) \times 100 \quad (2)$$

where C_0 and C_t both in mg/L are, respectively, the initial and remaining concentration of MB in solution at time t (min).

The percentage of COD removal was calculated by the following equation:

$$\text{COD removal (\%)} = \left(\frac{D_0 - D_t}{D_0} \right) \times 100 \quad (3)$$

where D_0 and D_t are the initial COD concentration (mg/L) and the COD concentration at time t (mg/L), respectively.

2.5. Experimental design

In the present study, an FCCD was employed to evaluate the combined effect of three independent variables at three levels namely initial pH (3–8), temperature (298–323 K), adsorbent dose (0.2–1.5 g/L), and contact time (15–90 min) on the color removal and COD reduction of MB. After selection of process (independent) variables, experiments were established based on an FCCD and the complete design consists of 30 experiments with 8 axial, 16 factorial and 6 center points. The center point was used to estimate the experimental error and repeated three times. Considering the general function expressing the interaction between the independent and dependent variables a second-order model was employed [13,26]:

$$y = \beta_0 + \sum_{i=1}^k \beta_i \chi_i + \sum_{i=1}^k \beta_{ii} \chi_i^2 + \sum_{i=1}^k \sum_{j \neq i}^k \beta_{ij} \chi_i \chi_j + \varepsilon \quad (4)$$

where y is the response (dependent variables); β_0 is the constant coefficient; β_i , β_{ii} and β_{ij} are the coefficients for the linear, quadratic and interaction coefficient, respectively; χ_i and χ_j are the coded values of variables and ε is the residual term. Regression coefficients of linear, quadratic and interaction involved in the model and their effects were analyzed by analysis of variance (ANOVA), and all the terms in the model were tested by student's F -test and significance of the F -values at probability levels ($p \leq 0.05$) were analyzed.

The experimental data was analyzed with various statistical analyses, such as sum of squares (SS), determination coefficient (R^2), adjusted determination of coefficient (R^2 -adj) and predicted determination of coefficient (R^2 -pred). All the statistical analyses were done by using a Stat ease

Design Expert 7.1.5 statistical software package (Stat-Ease Inc., Minneapolis, USA), and the developed mathematical models were used for the construction of contour and three-dimensional (3D) response surface plots in order to predict the relationships between independent and dependent variables. The numerical optimization technique was applied for validating the adequacy of the model equation for predicting the optimum response values. Verification experiments were performed under the optimal conditions, and the value of the experiments was compared with the predicted values of the developed model equations.

3. Results and discussion

3.1. CLs-AC characterization

The characteristics of prepared CLs-AC were determined and summarized in Table 1. The most important characteristic is iodine number, and the results showed that its value is 225.12 mg/g. This iodine number is a measure of micropore content (0–20 Å). The pH_{pzc} for CLs-AC was determined to be 7.70 as shown in Fig. 1; this value is the point where $\text{pH}_i = \text{pH}_f$. Therefore, the net charge in the CLs-AC surface is zero on condition that the solution approaches $\text{pH} = 7.70$. The surface morphology of CLs-AC was observed using an SEM technique. Fig. 2(a) shows the surface morphology of CLs-AC powder before MB adsorption. The CLs-AC material showed a rough, uneven and discontinuous surface with a high porous structure. The surface condition of CLs-AC was responsible for its good adsorption property. After MB adsorption, the surface of the dye-loaded CLs-AC displayed an irregular, wavy, non-porous, and compact structure because

Table 1
Characteristics of prepared activated carbon, CLs-AC

Characteristic	Value
Iodine number, mg/g	225.1
pH_{pzc}	7.70
Bulk density, g/mL	0.11
Moisture content, %	6.5
Ash content, %	26.7

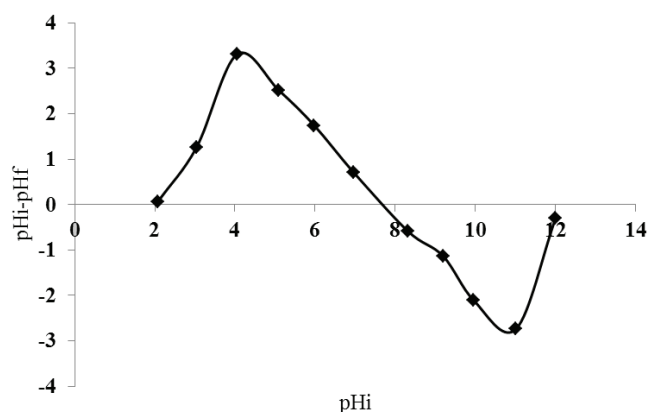


Fig. 1. pH_{pzc} of CLs-AC.

of the adsorbed MB dye molecules as shown in Fig. 2(b). FTIR analysis was performed to identify the main functional groups in CLs-AC that may be involved in the adsorption process. The FTIR spectra of the CLs-AC before and after MB adsorption are shown in Figs. 3(a) and (b), respectively. From Fig. 3(a), a number of absorption peaks were observed, indicating the complex nature of the prepared CLs-AC. The results indicated sorbent heterogeneity, evidenced by the different characteristic bands. The main functional groups are 3411.08 cm^{-1} for bonded $-\text{OH}$ groups, 1597.55 cm^{-1} for $\text{C}=\text{C}$ stretching, 1413.26 cm^{-1} for $\text{C}-\text{O}$ stretching, 1159.89 cm^{-1} for $\text{C}-\text{N}$ stretching, 1047.24 cm^{-1} for $\text{H}-\text{C}=\text{O}$ bending of aliphatic aldehydes, and 710.92 cm^{-1} for $\text{C}-\text{Cl}$ stretching. After MB adsorption, Fig. 2(b) shows some shift in the functional groups, disappear, and new peaks are appeared after the sorption of MB. This indicates the possible involvement of the functional groups during the adsorption process [26].

3.2. Screening experiment

In this study, four factors namely pH (factor A), temperature (factor B), adsorbent dose (factor C) and contact time (factor D) with three levels of FCCD were used to

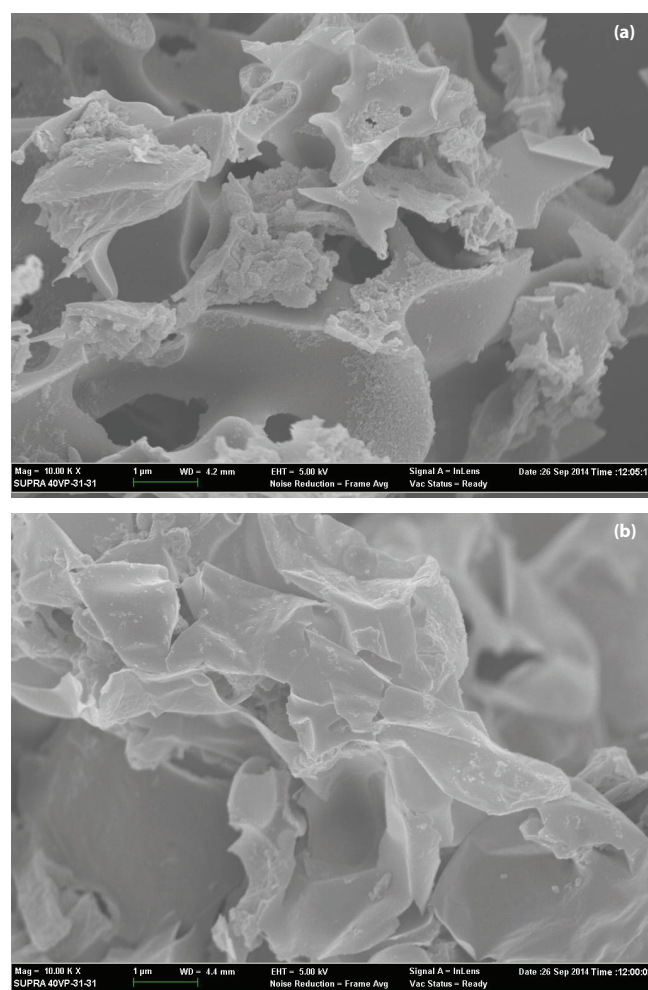


Fig. 2. SEM images of CLs-AC before adsorption (a) and after MB adsorption (b) at magnification 10.00 KX.

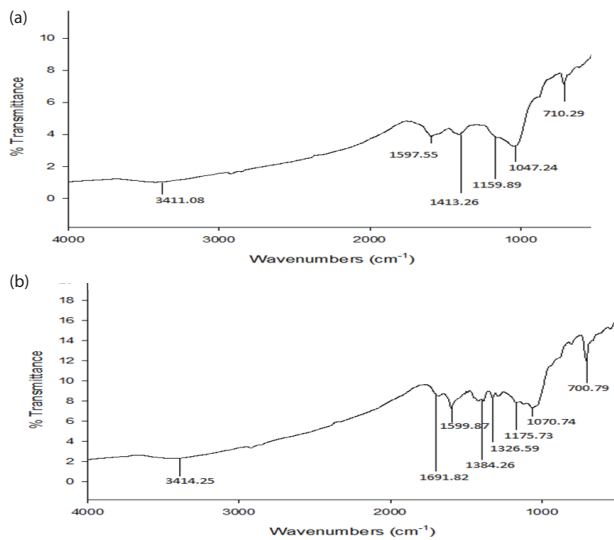


Fig. 3. FTIR spectra of CLs-AC before adsorption (a) and after MB adsorption (b).

evaluate the effect and optimize the process variables on the responses such as color removal and COD reduction of MB dye from an aqueous solution using CLs-AC as adsorbent. A total number of 30 batch experiments including six center points were performed in triplicates using statistically designed experiments (FCCD), and the results are shown in Table 2.

3.3. Statistical analysis

The experimental results were analyzed statistically by ANOVA. Significance of the developed model equations was evaluated by their corresponding F - and p -values, and it is shown in Table 3. Values of model terms $\text{Prob} > F < 0.0500$ indicate that factors are significant under selected conditions. This plays an important role in the design of experiment as it represents the significance of the terms in the model onto the responses being studied [49]. Significant model terms for MB color removal and COD reduction responses are A, B, C, D, BD, CD, A², C² and D². The other remaining terms had less significance for the response and could be neglected to

Table 2
FCCD and their experimental results

Run	A	B	C	D	Color removal		COD removal	
					% Y ₁	% X ₁	% Y ₂	% X ₂
1	3	298	0.20	15	30.82	30.51	29.73	29.23
2	8	298	0.20	15	35.42	35.88	33.23	34.23
3	3	323	0.20	15	53.29	53.91	50.73	52.22
4	8	323	0.20	15	58.87	58.47	56.72	55.20
5	3	298	1.50	15	44.37	45.58	42.77	43.09
6	8	298	1.50	15	50.93	51.78	49.32	50.61
7	3	323	1.50	15	65.94	65.61	64.11	64.18
8	8	323	1.50	15	70.33	71.01	68.99	69.67
9	3	298	0.20	90	61.45	61.72	59.57	59.74
10	8	298	0.20	90	64.88	65.81	64.01	64.41
11	3	323	0.20	90	75.70	75.45	73.82	73.00
12	8	323	0.20	90	79.02	78.74	75.11	75.64
13	3	298	1.50	90	84.79	85.79	80.47	82.45
14	8	298	1.50	90	90.40	90.72	90.26	89.62
15	3	323	1.50	90	95.67	96.15	93.94	93.79
16	8	323	1.50	90	99.37	100.28	97.99	98.95
17	3	310.5	0.85	52.5	85.19	82.49	84.15	81.59
18	8	310.5	0.85	52.5	90.71	87.24	89.37	86.66
19	5.5	298	0.85	52.5	77.51	72.77	75.99	71.96
20	5.5	323	0.85	52.5	90.67	89.25	89.35	88.11
21	5.5	310.5	0.20	52.5	65.09	64.04	63.22	62.46
22	5.5	310.5	1.50	52.5	87.46	82.34	85.55	81.04
23	5.5	310.5	0.85	15	48.28	45.50	45.85	43.01
24	5.5	310.5	0.85	90	79.12	75.74	75.33	72.90
25	5.5	310.5	0.85	52.5	74.13	77.66	74.01	76.37
26	5.5	310.5	0.85	52.5	74.01	77.66	72.79	76.37
27	5.5	310.5	0.85	52.5	75.75	77.66	73.54	76.37
28	5.5	310.5	0.85	52.5	74.45	77.66	72.74	76.37
29	5.5	310.5	0.85	52.5	73.72	77.66	74.33	76.37
30	5.5	310.5	0.85	52.5	75.38	77.66	75.01	76.37

Note: A = pH, B = temperature (K), C = adsorbent dose (g), D = contact time (min), Y = actual percentage (%), and X = predicted percentage (%).

Table 3
ANOVA table for responses

Source	DF	Color removal				COD removal			
		Sum of squares	Mean of square	F-value	Prob > F	Sum of squares	Mean of square	F-value	Prob > F
Model	14	8,531.09	609.36	62.86	<0.0001	8,485.59	606.11	73.36	<0.0001
A	1	101.33	101.3	10.45	0.0056	126.46	126.46	15.30	0.0014
B	1	1,221.98	1,221.98	126.06	<0.0001	1,142.58	1,142.58	138.28	<0.0001
C	1	1,507.59	1,507.59	155.52	<0.0001	1,517.27	1,517.27	183.63	<0.0001
D	1	4,115.33	4,115.33	424.54	<0.0001	3,961.98	3,961.98	479.50	<0.0001
AB	1	0.64	0.64	0.066	0.8000	6.34	6.34	0.77	0.3949
AC	1	0.70	0.70	0.072	0.7923	4.05	4.05	0.49	0.4946
AD	1	1.62	1.62	0.17	0.6884	0.70	0.70	0.085	0.7748
BC	1	11.36	11.36	1.17	0.2962	1.98	1.98	0.24	0.6315
BD	1	93.42	93.42	9.64	0.0073	85.33	85.33	10.33	0.0058
CD	1	80.98	80.98	8.35	0.0112	87.28	87.28	10.56	0.0054
A ²	1	132.71	132.71	13.69	0.0021	157.19	157.19	19.02	0.0006
B ²	1	28.20	28.20	2.91	0.1087	35.45	35.45	4.29	0.0560
C ²	1	52.94	52.94	5.46	0.0337	54.49	54.49	6.59	0.0214
D ²	1	756.71	756.71	78.06	<0.0001	875.36	875.36	105.94	<0.0001
Residual	15	145.40	9.69			123.94	8.26		
Pure error	5	3.21	0.64			3.98	0.80		
Cor. total	29	8,676.49				8,609.53			

Note: A = pH, B = Temperature, C = Adsorbent dose, and D = contact time.

Color removal: $R^2 = 0.9832$, Adj $R^2 = 0.9676$, and Pred $R^2 = 0.9493$.

COD removal: $R^2 = 0.9855$, Adj $R^2 = 0.9720$, and Pred $R^2 = 0.9508$.

improve the model. The developed empirical models in terms of coded factors for both color removal and COD reduction are expressed in Eqs. (5) and (6):

$$\begin{aligned} \text{Color removal } (Y_1) = & 77.85 + 2.37A + 8.24B + 9.15C \\ & + 15.12D - 2.42BD + 2.25CD \\ & + 7.16A^2 - 4.52C^2 - 17.09D^2 \end{aligned} \quad (5)$$

$$\begin{aligned} \text{COD reduction } (Y_2) = & 76.37 + 2.54A + 8.08B \\ & + 9.29C + 14.95D - 2.43BD \\ & + 2.21CD + 7.75A^2 - 4.62C^2 \end{aligned} \quad (6)$$

The goodness of fit of the models was evaluated by the determination coefficient (R^2), adjusted determination coefficient (R^2 -adj) and predicted determination coefficient (R^2 -pred). The high R^2 , R^2 -adj and R^2 -pred values for both color removal and COD reduction (Table 3) revealed that the models are statistically significant and only small variations are not explained by the models.

3.4. Adequacy of developed mathematical models

The adequacy of developed mathematical models was evaluated by constructing diagnostic plots such as predicted vs. actual and normal probability plots for the experimental data obtained from this study. The normal probability plots show whether the residuals follow a normal distribution, in which case the points will follow a straight line [50]. The plot

of normal probability of the residual for color removal and COD reduction are depicted in Figs. 4(a) and (b), respectively. The trend reveals a reasonably well-behaved residual vs. the expected values, and the residual is normally distributed as a straight line and shows no deviation of variance. This can confirm the normal distribution of the observed data and adequacy of the developed models. Diagnostic plots of predicted vs. actual responses for color removal and COD reduction are shown in Figs. 5(a) and (b), respectively. These figures assist us to investigate the relationship between predicted and experimental values and evaluate the model suitability. From Figs. 5(a) and (b), it was observed that the data points on this plot lie very close to the diagonal line indicating a good agreement between experimental data and the values predicted by the developed models.

3.5. Effect of process variables

Perturbation plots and 3D response surface plots were plotted from the developed mathematical models in order to study the individual and interactive effects among the process variables on the responses and also used to determine the optimal condition of each factor for higher color removal and COD reduction of MB from aqueous solutions using CLs-AC.

3.5.1. Effect of independent variables

Perturbation plots was used to investigate the individual effect of the four independent variables, including pH (factor A), temperature (factor B), adsorbent dose (factor C)

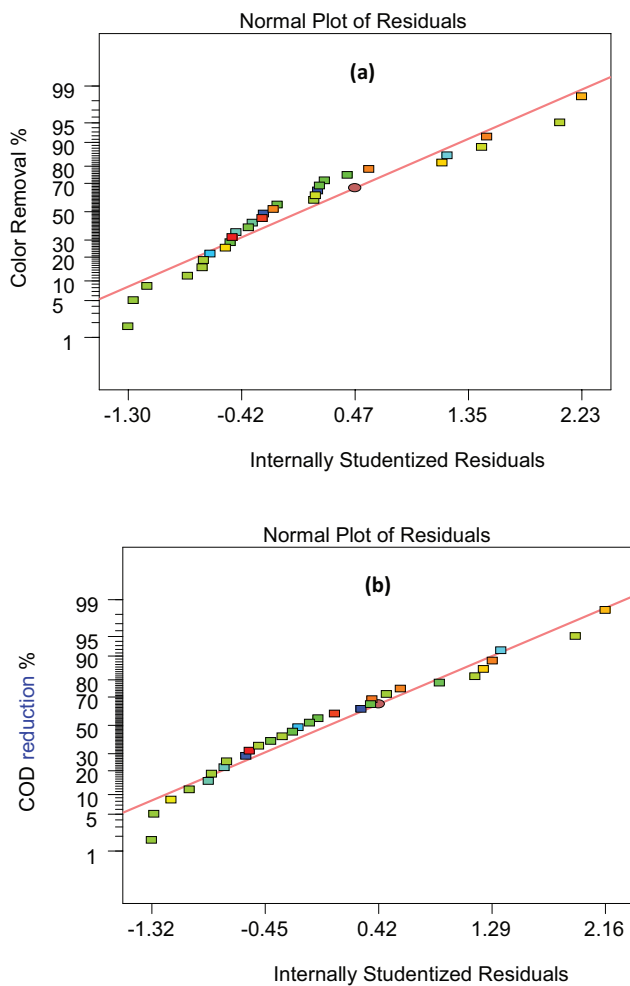


Fig. 4. Normal probability plot for responses of MB color removal (a) and COD reduction (b).

and time of agitation (factor D), on the MB removal. A perturbation plot employs the model terms to show the influence of each factor deviation from the reference point on the process response, while holding the other factors constant. Design-Expert software automatically sets the reference point at the midpoint (coded 0) of all the factors. The perturbation plot can be applied to find out the most significant factors on the response. A steep slope or curvature in a factor shows that the response is sensitive to that variable. A relatively flat line indicates response insensitivity to change in that particular variable [51]. Perturbation plots for the MB color removal and COD removal efficiencies are shown in Figs. 6(a) and (b), respectively. From Figs 6(a) and (b), it can conclude that the influence of studied variables was found to be nearly the same on the MB color removal and COD reduction responses. A sharp curvature for the independent variables namely temperature (B), adsorbent dose (C) and contact time (D) suggests that the responses of the MB color removal and COD removal efficiencies were very sensitive to these parameters. In general, it was observed that color removal and COD removal efficiencies increased slightly with increasing the solution pH (A) toward basic environment. At a solution pH

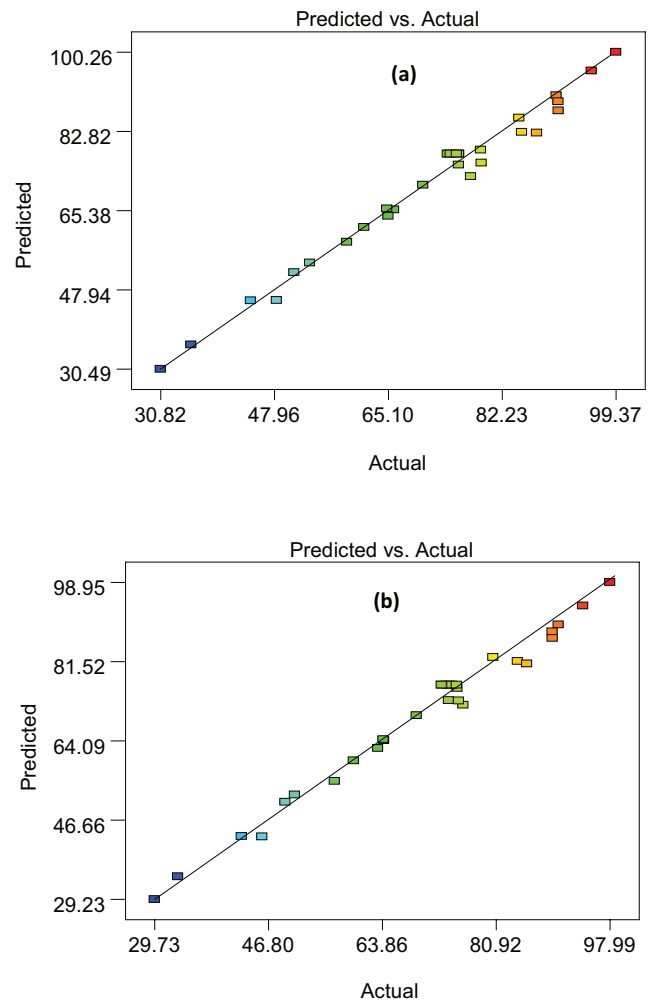


Fig. 5. Diagnostic plots for model adequacy of MB color removal (a) and COD reduction (b).

higher than pH_{pzc} ($\text{pH}_{\text{pzc}} = 7.70$ as recorded in Table 1), the CLS-AC surface has negative charge, and electrostatic attraction between negative surface and positive functional groups of MB is favorable, while CLS-AC will react as a positive surface when the solution pH is lower than pH_{pzc} [52].

3.5.2. Interaction effects on responses and process optimization

ANOVA results for the response parameter (Table 3) indicated that the maximum color removal and COD reduction can be obtained by only BD and CD interactions. Figs. 7 and 8 show the 3D plots of the responses at the optimal interaction terms of BD and CD, respectively, and simultaneously keeping the other two variables constant at central level. In Figs 7(a) and (b), the response surface was developed as a function of temperature (B) and contact time (D) while the solution pH (A) and adsorbent dose (C) were kept constant at 5.50 and 0.85 g/L, respectively. As can be seen, the color removal and COD reduction increased with increasing in temperature and contact time. With the change in temperature, CLS-AC pore structure changes, which accounts for the variation in color removal and

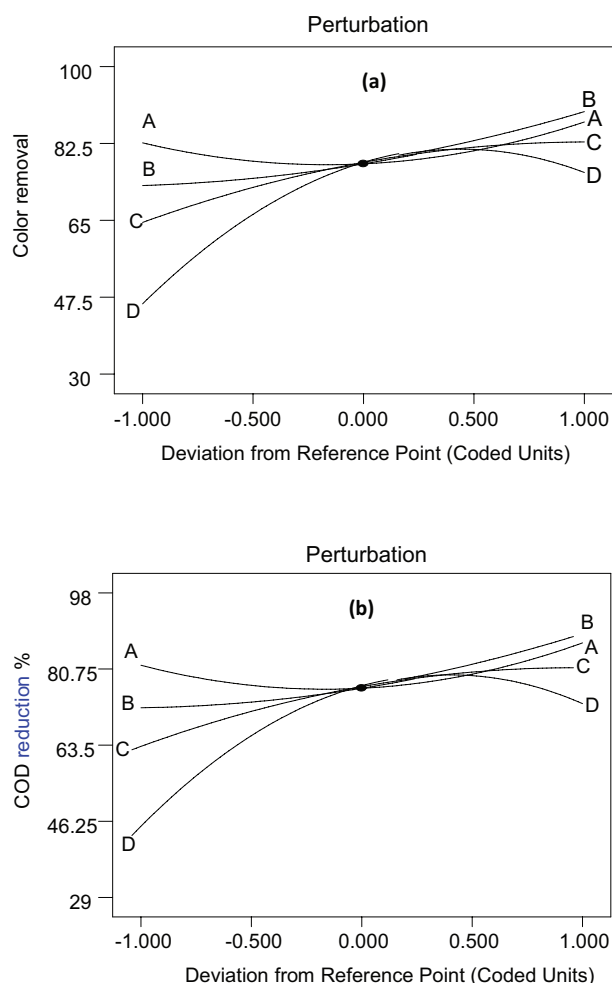


Fig. 6. Perturbation plots of MB color removal (a) and COD reduction (b) by AC-CLs.

COD reduction of MB. This increase in MB removal may be due to the increase in mobility of MB molecules and increase in the equilibrium constant. This showed the endothermic nature of adsorption. Time of agitation offers better contact between the dye and CLs-AC particles. The percentage of color removal and COD reduction increased rapidly by increasing agitation time up to 71.25 min. Longer agitation time allows the MB molecules more chances to penetrate into the interior surface of CLs-AC adsorbent pore after the adsorption sites available on the exterior surface of the CLs-AC particles are occupied during the first period of agitation time. However, no remarkable change was observed in color removal and COD reduction after reaching 71.25 min, and further increase in contact time does not bring significant change. This indicates that the adsorption process reached equilibrium with this period of time and remained stable by increasing contact time. The interaction effect of adsorbent dose (C) and contact time (D) on color removal and COD reduction at fixed temperature 310.50 K and solution pH 5.50 is shown in the 3D plots of Figs. 8(a) and (b), respectively. Adsorbent dose reveals the ability of the CLs-AC adsorbent to uptake MB molecules from a given solution. Therefore, the color removal and COD reduction increased with simultaneous increase in adsorbent dose. In

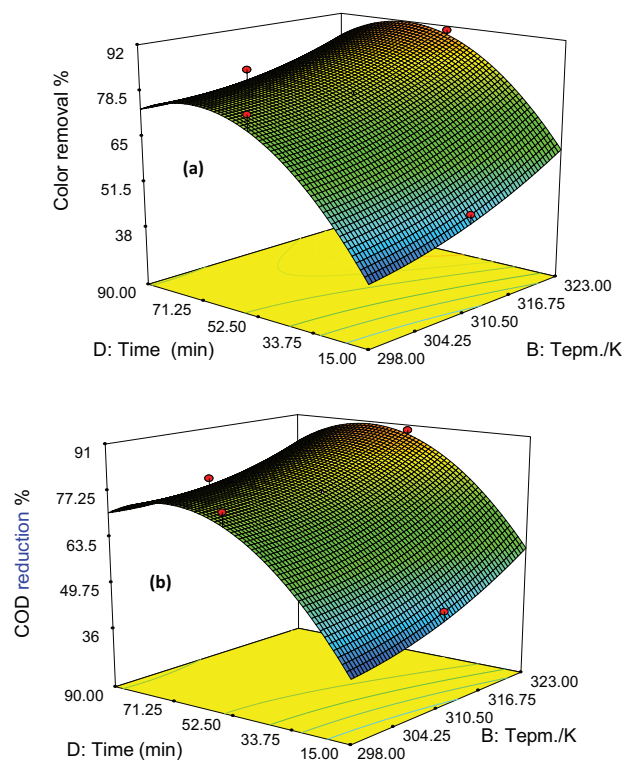


Fig. 7. Effect of process variables (B and D) on responses of color removal (a) and of COD reduction (b).

general, increasing the adsorbent dose provides greater surface area and increases the availability of binding sites [53].

3.6. Confirmation experiment

Conformity experiment was carried out on the predicted responses obtained from the software by using numerical modeling under optimized conditions. At the initial concentration of MB dye 100 mg/L, the optimum predicted conditions identified were initial solution pH of 3.07, temperature 322.70 K, CLs-AC dose 1.20 g/L and contact time of 70.62 min. The predicted values of color removal and COD removal were 99.37% and 98.27%, respectively. The actual values of color removal and COD reduction achieved were 97.03% and 95.42%, respectively. This observation indicates that the deviation of predicted percentage removal and actual percentage removal was less. However, in order to avoid the competition effect of H_3O^+ ions with dye molecules at acidic environment, additional cost caused by pH control and unfavorable characteristic of acidic environment for real wastewater decolorization. Therefore, the optimal experimental conditions given in Table 2, initial solution pH of 8.00, temperature 323.00 K and CLs-AC dose 1.50 g/L were adopted for all the following adsorption studies.

3.7. Effect of initial MB dye concentration

The equilibrium contact time is crucial for determining the adsorption capacity of the adsorbents. The adsorbed amount of MB at time t , q_t (mg/g), was calculated as follows:

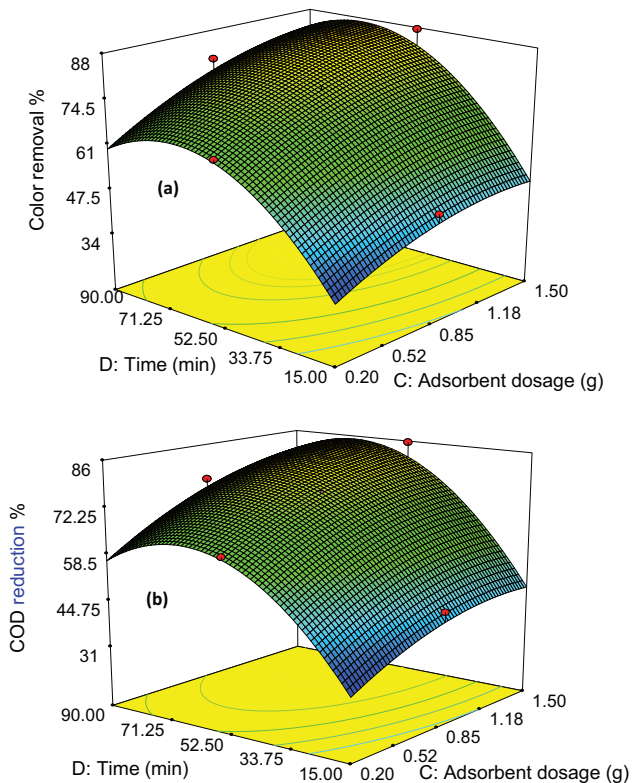


Fig. 8. Effect of process variables (C and D) on responses of color removal (a) and of COD reduction (b).

$$q_t = \frac{(C_0 - C_t)V}{W} \quad (7)$$

where C_t (mg/L) is the liquid-phase concentration of MB solution at time t (min). Adsorption capacity, q_t , as a function of time, t , at different initial MB concentrations is shown in Fig. 9. The adsorption capacities of MB dye on CLs-AC increased with increasing the contact time. It is obvious from Fig. 9 that the adsorption process increased sharply at the initial stage indicating the availability of readily accessible sites on CLs-AC surface. The process became gradually slower as equilibrium attended. This phenomenon is attributed to the reduction of immediate solute adsorption due to the lack of available open sites for dye adsorption, which in turn supported film diffusion [54]. At this point, the amount of dye desorbing from the adsorbent is in a state of dynamic equilibrium with the amount of dye being adsorbed onto the AC. The time required to attain this state of equilibrium is termed as equilibrium time. Initial concentration provides an essential driving force to overcome the mass transfer resistance between the aqueous phase and the solid medium [55]. In the present research, adsorption equilibrium, q_e , increased from 25.80 to 87.04 mg/g with an increase in initial concentration from 20 to 100 mg/L. A similar observation was reported by Foo and Hameed [32] for the uptake of MB on the surface of AC prepared from jackfruit peel by microwave induced NaOH activation.

3.8. Adsorption isotherm studies

Adsorption isotherm is an essential data source for practical design and fundamental understanding of carbonaceous adsorbents. Typically, the mathematical correlation is accessed by linear regression analysis. To determine the adsorption capacity of CLs-AC for the removal of MB dye from aqueous solutions, different forms of isotherm equations namely Langmuir, Freundlich and Temkin isotherm models were tested. The Langmuir model (Eq. (8)) assumes that the adsorptions occur at specific homogeneous sites on the adsorbent. This model is successfully used in numerous monolayer adsorption processes [56]:

$$\frac{C_e}{q_e} = \frac{1}{q_m K_L} + \frac{1}{q_m} C_e \quad (8)$$

where C_e is the equilibrium concentration (mg/L); q_e is the amount adsorbed per specified amount of adsorbent (mg/g); K_L is the Langmuir equilibrium constant and q_m is the amount of adsorbate required to form a monolayer. The Freundlich model (Eq. (9)) can be applied for non-ideal adsorption on heterogeneous surfaces and multilayer adsorption [57]:

$$\ln q_e = \ln K_F + \frac{1}{n} \ln C_e \quad (9)$$

where K_F is the Freundlich equilibrium constant; n is an empirical constant and the rest of the terms have the usual significance. In addition, Temkin model (Eq. (10)) considers the effects of indirect adsorbate/adsorbate interactions on adsorption isotherms [58]:

$$q_e = B \ln K_T + B \ln C_e \quad (10)$$

where K_T is the Temkin equilibrium binding constant (L/mg) that corresponds to the maximum binding energy, and constant B is related to adsorption heat. The adsorption heat of all the molecules in the layer is expected to decrease linearly with coverage because of adsorbate/adsorbate interactions. The obtained isotherm constants for the three isotherms models and their corresponding R^2 are recorded in Table 4. The Langmuir model fit the data better than the

Table 4
Isotherm parameters for MB adsorption on CLs-AC surface (CLs-AC dose = 0.15 g, V = 0.1 L; pH = 8.00; and T = 323 K).

Isotherm	Parameter	Value
Langmuir	q_m (mg/g)	87.72
	K_L (L/mg)	0.59
	R^2	0.9907
Freundlich	K_F ((mg/g) (L/mg) ^{1/n})	0.0039
	n	0.27
	R^2	0.8018
Temkin	K_T (L/mg)	9.52
	B	15.90
	R^2	0.9731

Table 5
Comparison adsorption capacities of various activated carbons for MB

Adsorbent	Adsorbent dosage, (g)	pH	Temp. (K)	Activation method/activator	q_{\max} (mg/g)	References
Coconut leaves	1.5 g/L	8	323	Microwave/NaOH	87.72	This study
Rice straw	0.1 g/0.1 L	–	298	Thermochemical/ $(\text{NH}_4)_2\text{HPO}_4$	129.00	[59]
Waste apricot	0.1 g/0.05 L	–	303–323	Thermochemical/ ZnCl_2	102.04–136.48	[60]
Wood apple rind	0.1 g/0.05 L	9	–	Thermochemical/ H_2SO_4	40.1	[61]
Sunflower cake	0.02 g/0.01 L	6	298	Thermochemical/ H_2SO_4	16.43	[62]
Coffee press cake	20 g/1 L	5	–	Thermophysical	14.27	[63]
Corn cob	0.02 g/0.1 L	8	298	Thermochemical/ H_3PO_4	28.65	[64]

Table 6
Kinetic parameters for MB adsorption on CLs-AC at 323 K

C_0 (mg/L)	Pseudo-first-order model			
	$q_{e,\text{exp}}$ (mg/g)	$q_{e,\text{cal}}$ (mg/g)	K_1 (1/min)	R^2
20	25.80	11.62	0.0784	0.7656
40	45.8645	23.5093	0.04111	0.7907
60	56.4813	32.9799	0.0548	0.8468
80	73.1121	67.2488	0.0961	0.9841
100	87.0467	108.3969	0.0901	0.9670
	Pseudo-second-order model			
	$q_{e,\text{exp}}$ (mg/g)	$q_{e,\text{cal}}$ (mg/g)	K_2 (g/mg min)	R^2
20	25.80	27.4725	0.0087	0.9812
40	45.8645	47.1698	0.0045	0.9825
60	56.4813	59.8802	0.0032	0.9837
80	73.1121	78.7401	0.0025	0.9863
100	87.0467	90.0900	0.0020	0.9855
	Intraparticle diffusion model			
	$q_{e,\text{exp}}$ (mg/g)	C (mg/g)	K_3 (mg/g min ^{1/2})	R^2
20	25.80	24.777	0.0926	0.8077
40	45.8645	39.063	0.547	0.9622
60	56.4813	52.998	0.2861	0.9324
80	73.1121	72.09	0.0922	0.8627
100	87.0467	80.514	0.6157	

Freundlich and Temkin models (Table 4). This result is also confirmed by the high R^2 value for the Langmuir model (0.9907) compared with the Temkin (0.9731) and Freundlich (0.8018) models. Therefore, the adsorption of MB on CLs-AC occurs as monolayer adsorption on a surface that is homogeneous in adsorption affinity. The obtained maximum monolayer adsorption capacity (q_m) of CLs-AC for MB was 87.72 mg/g (Table 4). Various types of adsorbents have been tested for their feasibility to remove MB dye from aqueous solutions. A comparative study of the MB adsorption onto AC prepared from various biomass precursors is provided in Table 5.

3.9. MB adsorption kinetics

The pseudo-first-order model [65], pseudo-second-order model [66] and intraparticle diffusion model [67] were used to investigate the adsorption kinetics of MB dye on CLs-AC. These models can be expressed as follows:

$$\text{Pseudo-first order model: } \ln(q_e - q) = \ln(q_e) - (k_1)t \quad (11)$$

$$\text{Pseudo-second order model: } \frac{t}{q} = \left(\frac{1}{k_2 q_e^2} \right) + \left(\frac{1}{q_e} \right) t \quad (12)$$

$$\text{Intraparticle diffusion model: } q_t = k_3 t^{1/2} + C \quad (13)$$

where q_e and q_t (mg/g) are the uptake of MB at equilibrium and at time t (min), respectively; k_1 (1/min) is the adsorption rate constant; k_2 (g/mg min) is the rate constant of second-order equation; k_3 (mg/g min^{1/2}) is the intraparticle diffusion rate constant, and C (mg/g) is a constant that gives an idea about the thickness of the boundary layer. The calculated constants of the three isotherm equations along with R^2 values at different initial MB concentrations are presented in Table 6. The linear plot of $\ln(q_e - q_t)$ vs. t (Fig. 10) for pseudo-first-order equation is of low R^2 value, as shown in Table 4. Moreover, this table shows a large difference between the experimental and calculated adsorption capacity, indicating a poor pseudo-first-order fit to the experimental data. High R^2 value is obtained for the linear plot of t/q_t vs. t (Fig. 11) for pseudo-second-order equation, as shown in Table 4. It can be seen that the pseudo-second-order kinetic model better represented the adsorption kinetics, and the calculated q_e values agree well with the experimental q_e values (Table 6). This indicates that the adsorption of MB on CLs-AC follows second-order kinetics. A similar result was reported by Foo and Hameed [31] for the adsorption of MB on AC produced from jackfruit peel by microwave-induced NaOH activation. From Table 6, the values of rate constant k_2 decrease with increasing initial concentration of MB. The reason for this behavior can be attributed to the high competition for the sorption surface sites at high concentration, which leads to higher sorption rates. On the other hand, for the intraparticle diffusion model, the low values of R^2 (Table 6) for the linear plot of q_t vs. $t^{1/2}$ (Fig. 12) indicate that this model could not fit properly the experimental kinetic data.

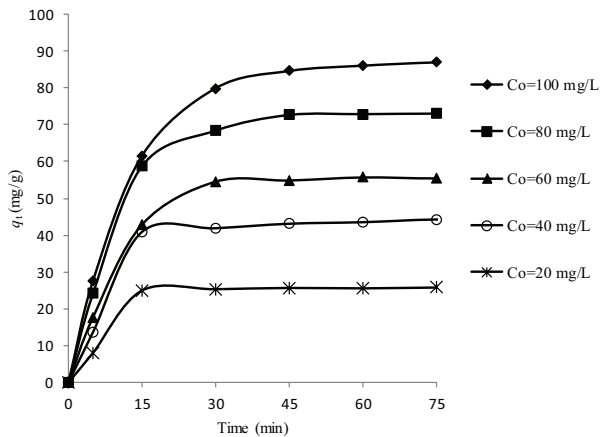


Fig. 9. Effect of initial concentration and contact time on the adsorption capacity of MB onto CLs-AC surface (CLs-AC dose = 0.15 g, $V = 0.1$ L; pH = 8.00; and $T = 323$ K).

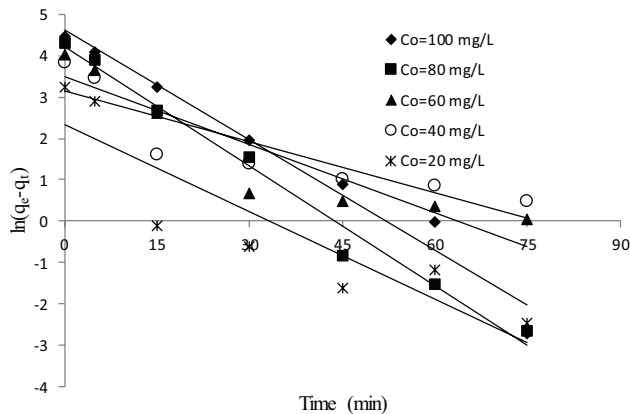


Fig. 10. Pseudo-first-order kinetic for MB adsorption on CLs-AC at different initial concentrations (CLs-AC dose = 0.15 g, $V = 0.1$ L; pH = 8.00; and $T = 323$ K).

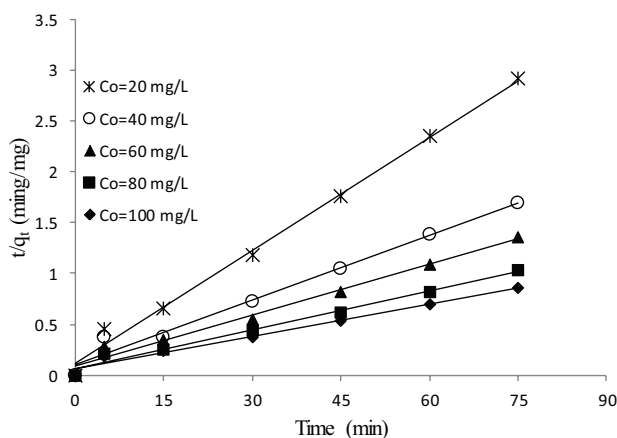


Fig. 11. Pseudo-second-order kinetic for MB adsorption on CLs-AC at different initial concentrations (CLs-AC dose = 0.15 g, $V = 0.1$ L; pH = 8.00; and $T = 323$ K).

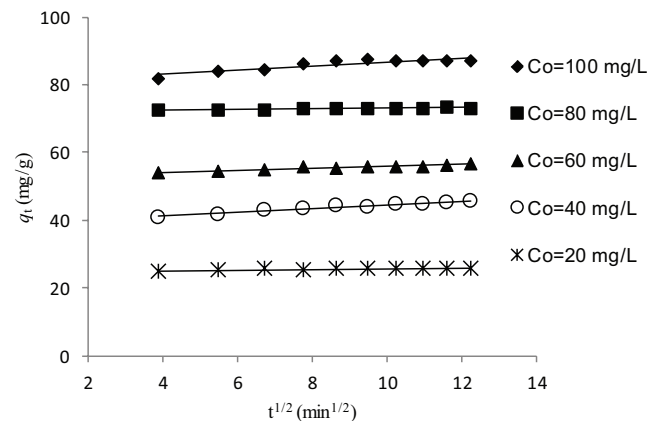


Fig. 12. Intraparticle diffusion plot for MB adsorption on CLs-AC at different initial concentrations (CLs-AC dose = 0.15 g, $V = 0.1$ L; pH = 8.00; and $T = 323$ K).

4. Conclusion

The present study utilizes an agricultural solid waste such as coconut leaves as precursor to produce AC (CLs-AC) for color removal and COD reduction of MB from its aqueous solution. RSM and the FCCD were appreciable in determining the optimal conditions for adsorption including pH, temperature, adsorbent dose, and contact time. The quadratic model was developed for process optimization, and statistical experimental designs were found to be useful tool for predicting and understanding the interaction effects between process parameters. The 3D response plots showed clear peaks for both responses, which means that the optimum conditions for maximum color removal and COD reduction are well defined inside the design boundary. The maximum color removal and COD reduction achieved were 99.37% and 98.27%, respectively, at 8.00 pH, 323.00 K temperature, 1.50 g/L adsorbent dose and 90 min contact. Under these optimal experimental conditions, the adsorption of MB dye followed the pseudo-second-order model. The equilibrium data fit very well in the Langmuir isotherm equation, confirming the monolayer adsorption capacity of MB dye onto CLs-AC with a monolayer adsorption capacity of 87.72 mg/g at 323.00 K. CLs-AC proved to be economically feasible and competent for the removal of basic dye from aqueous solutions.

Acknowledgment

The authors would like to thank the Chemistry department, Faculty of applied sciences, Universiti Teknologi MARA, Arau Campus for facilitating this research work.

References

- [1] N.S.A. Mubarak, A.H. Jawad, W.I. Nawawi, Equilibrium, kinetic and thermodynamic studies of Reactive Red 120 dye adsorption by chitosan beads from aqueous solution, *Energ. Ecol. Environ.* (2016) 1–9. doi: 10.1007/s40974-016-0027-6
- [2] L.W. Low, T.T. Teng, N. Morad, B. Azahari, Studies on the adsorption of methylene blue dye from aqueous solution onto low-cost tartaric acid treated bagasse, *APCBEE Procedia*, 1 (2012) 103–109.

- [3] A.H. Jawad, R.A. Rashid, M.A.M. Ishak, L.D. Wilson, Adsorption of methylene blue onto activated carbon developed from biomass waste by H_2SO_4 activation: kinetic, equilibrium and thermodynamic studies, *Desal. Wat. Treat.*, 57 (2016) 25194–25206.
- [4] R.A. Rashid, A.H. Jawad, M.A.M. Ishak, N.N. Kasim, KOH-activated carbon developed from biomass waste: adsorption equilibrium, kinetic and thermodynamic studies for methylene blue uptake, *Desal. Wat. Treat.*, 57 (2016) 27226–27236.
- [5] I.A.W. Tan, A.L. Ahmad, B.H. Hameed, Enhancement of basic dye adsorption uptake from aqueous solutions using chemically modified oil palm shell activated carbon, *Colloids Surf., A*, 318 (2008) 88–96.
- [6] E.N. El Qada, S.J. Allen, G.M. Walker, Adsorption of methylene blue onto activated carbon produced from steam activated bituminous coal: a study of equilibrium adsorption isotherm, *Chem. Eng. J.*, 124 (2006) 103–110.
- [7] L.W. Low, T.T. Teng, A. Ahmad, N. Morad, Y.S. Wong, A novel pretreatment method of lignocellulosic material as adsorbent and kinetic study of dye waste adsorption, *Water Air Soil Pollut.*, 218 (2011) 293–306.
- [8] S. Senthilkumar, P.R. Varadarajan, K. Porkodi, C.V. Subbhuraam, Adsorption of methylene blue onto jute fiber carbon: kinetics and equilibrium studies, *J. Colloid Interface Sci.*, 284 (2005) 78–82.
- [9] A. Khataee, A. Movafeghi, S. Torbati, S.S. Lisar, M. Zarei, Phytoremediation potential of duckweed (*Lemna minor* L.) in degradation of CI Acid Blue 92: artificial neural network modeling, *Ecotoxicol. Environ. Saf.*, 80 (2012) 291–298.
- [10] L. Fan, Y. Zhou, W. Yang, G. Chen, F. Yang, Electrochemical degradation of aqueous solution of amaranth azo dye on ACF under potentiostatic model, *Dyes Pigment.*, 76 (2008) 440–446.
- [11] J.-S. Wu, C.-H. Liu, K.H. Chu, S.-Y. Suen, Removal of cationic dye methyl violet 2B from water by cation exchange membranes, *J. Membr. Sci.*, 309 (2008) 239–245.
- [12] Y.S. Woo, M. Rafatullah, A.F.M. Al-Karkhi, T.T. Tow, Removal of Terasil Red R dye by using Fenton oxidation: a statistical analysis, *Desal. Wat. Treat.*, 52 (2014) 4583–4591.
- [13] A.H. Jawad, A.F. Alkarkhi, N.S.A. Mubarak, Photocatalytic decolorization of methylene blue by an immobilized TiO_2 film under visible light irradiation: optimization using response surface methodology (RSM), *Desal. Wat. Treat.*, 56 (2015) 161–172.
- [14] A.H. Jawad, N.S.A. Mubarak, M.A.M. Ishak, K. Ismail, W. Nawawi, Kinetics of photocatalytic decolorization of cationic dye using porous TiO_2 film, *J. Taibah Univ. Sci.*, 10 (2016) 352–362.
- [15] A.H. Jawad, M.A. Nawi, Characterizations of the photocatalytically-oxidized cross-linked chitosan-glutaraldehyde and its application as a sub-layer in the TiO_2 /CS-GLA bilayer photocatalyst system, *J. Polym. Environ.*, 20 (2012) 817–829.
- [16] C.X.H. Su, T.T. Teng, A.F.M. Alkarkhi, L.W. Low, *Imperata cylindrica* (Cogongrass) as an adsorbent for methylene blue dye removal: process optimization, *Water Air Soil Pollut.*, 225 (2014) 1–12.
- [16] A. Gurses, A. Hassani, M. Kiransan, O. Acisli, S. Karaca, Removal of methylene blue from aqueous solution by using untreated lignite as potential low-cost adsorbent: kinetic, thermodynamic and equilibrium approach, *J. Water Process Eng.*, 2 (2014) 10–21.
- [17] M.A. Khan, B.H. Hameed, J. Lawler, M. Kumar, B.H. Jeon, Developments in activated functionalized carbons and their applications in water decontamination: a review, *Desal. Wat. Treat.*, 54 (2015) 422–449.
- [18] C. Saka, Ö. Sahin, Removal of methylene blue from aqueous solutions by using cold plasma- and formaldehyde-treated onion skins, *Color. Technol.*, 127 (2011) 246–255.
- [19] L.W. Low, T.T. Teng, N. Morad, B. Azahari, Optimization of the column studies into the adsorption of basic dye using tartaric acid-treated bagasse, *Desal. Wat. Treat.*, 52 (2014) 6194–6205.
- [20] Ö. Sahin, C. Saka, Preparation and characterization of activated carbon from acorn shell by physical activation with H_2O - CO_2 in two-step pretreatment, *Bioresour. Technol.*, 136 (2013) 163–168.
- [21] M. Özdemir, T. Bolgaz, C. Saka, Ö. Sahin, Preparation and characterization of activated carbon from cotton stalks in a two-stage process, *J. Anal. Appl. Pyrolysis*, 92 (2011) 171–175.
- [22] C. Saka, BET, TG–DTG, FT-IR, SEM, iodine number analysis and preparation of activated carbon from acorn shell by chemical activation with $ZnCl_2$, *J. Anal. Appl. Pyrolysis*, 95 (2012) 21–24.
- [23] A. Özhan, Ö. Sahin, M.M. Küçük, C. Saka, Preparation and characterization of activated carbon from pine cone by microwave-induced $ZnCl_2$ activation and its effects on the adsorption of methylene blue, *Cellulose*, 21 (2014) 2457–2467.
- [24] M. Oghbaei, O. Mirzaee, Microwave versus conventional sintering: a review of fundamentals, advantages and applications, *J. Alloys Compd.*, 494 (2010) 175–189.
- [25] P.J.M. Carrott, J.M.V. Nabais, M.M.L.R. Carrott, J.A. Menendez, Thermal treatments of activated carbon fibres using a microwave furnace, *Microporous Mesoporous Mater.*, 47 (2001) 243–252.
- [26] A.H. Jawad, R.A. Rashid, R.M.A. Mahmuod, M.A.M. Ishak, N.N. Kasim, K. Ismail, Adsorption of methylene blue onto coconut (*Cocos nucifera*) leaf: optimization, isotherm and kinetic studies, *Desal. Wat. Treat.*, 57 (2016) 8839–8853.
- [27] L. Khezami, A. Ould-Dris, R. Capart, Activated carbon from thermo-compressed wood and other lignocellulosic precursors, *BioResources*, 2 (2007) 193–209.
- [28] T. Kawano, M. Kubota, M.S. Onyango, F. Watanabe, H. Matsuda, Preparation of activated carbon from petroleum coke by KOH chemical activation for adsorption heat pump, *Appl. Therm. Eng.*, 28 (2008) 865–871.
- [29] A.L. Cazetta, A.M.M. Vargas, E.M. Nogami, M.H. Kunita, M.R. Guilherme, A.C. Martins, T.L. Silva, J.C.G. Moraes, V.C. Almeida, NaOH-activated carbon of high surface area produced from coconut shell: kinetics and equilibrium studies from the methylene blue adsorption, *Chem. Eng. J.*, 174 (2011) 117–125.
- [30] V.S. Mane, P.V.V. Babu, Studies on the adsorption of Brilliant Green dye from aqueous solution onto low-cost NaOH treated saw dust, *Desalination*, 273 (2011) 321–329.
- [31] K.Y. Foo, B.H. Hameed, Potential of jackfruit peel as precursor for activated carbon prepared by microwave induced NaOH activation, *Bioresour. Technol.*, 112 (2012) 143–150.
- [32] K.Y. Foo, B.H. Hameed, Textural porosity, surface chemistry and adsorptive properties of durian shell derived activated carbon prepared by microwave assisted NaOH activation, *Chem. Eng. J.*, 187 (2012) 53–62.
- [33] Y. Chen, S.R. Zhai, N. Liu, Y. Song, Q.D. An, X.W. Song, Dye removal of activated carbons prepared from NaOH-pretreated rice husks by low-temperature solution-processed carbonization and H_3PO_4 activation, *Bioresour. Technol.*, 144 (2013) 401–409.
- [34] L. Lin, S.R. Zhai, Z.Y. Xiao, Y. Song, Q.D. An, X.W. Song, Dye adsorption of mesoporous activated carbons produced from NaOH-pretreated rice husks, *Bioresour. Technol.*, 136 (2013) 437–443.
- [35] A.C. Martins, O. Pezoti, A.L. Cazetta, K.C. Bedin, D.A.S. Yamazaki, G.F.G. Bandoch, T. Asefa, J.V. Visentainer, V.C. Almeida, Removal of tetracycline by NaOH-activated carbon produced from macadamia nut shells: kinetic and equilibrium studies, *Chem. Eng. J.*, 260 (2015) 291–299.
- [36] R.L. Tseng, Mesopore control of high surface area NaOH-activated carbon, *J. Colloid Interface Sci.*, 303 (2006) 494–502.
- [37] D. Granato, G.F. Branco, V.M. Calado, Experimental design and application of response surface methodology for process modelling and optimization: a review, *Food Res. Int.*, 44 (2011) 1036–1043.
- [38] M.A. Bezerra, R.E. Santelli, E.P. Oliveira, L.S. Villar, L.A. Escalera, Response surface methodology (RSM) as a tool for optimization in analytical chemistry, *Talanta*, 76 (2008) 965–977.
- [39] M. Vepsäläinen, M. Ghiasvand, J. Selinc, J. Pienimaac, E. Repo, M. Pulliainen, M. Sillanpaa, Investigations of the effects of temperature and initial sample pH on natural organic matter (NOM) removal with electrocoagulation using response surface method (RSM), *Sep. Purif. Technol.*, 69 (2009) 255–261.
- [40] M.A. Jamaluddin, K. Ismail, M.A.M. Ishak, Z.A. Ghani, M.F. Abdullah, M.T.U. Safian, S.S. Idris, S. Tahiruddin, M.F.M. Yunus, N.I.N.M. Hakimi, Microwave-assisted pyrolysis of palm kernel shell: optimization using response surface methodology (RSM), *Renew. Energy*, 55 (2013) 357–365.

- [41] M. Auta, B.H. Hameed, Optimized waste tea activated carbon for adsorption of Methylene Blue and Acid Blue 29 dyes using response surface methodology, *Chem. Eng. J.*, 175 (2011) 233–243.
- [42] Lubrizol Standard Test Method, Iodine Value, Test Procedure AATM 1112-01, 2006.
- [43] M. Ahmedna, W.E. Marshall, R.M. Rao, S.J. Clarke, Use of filtration and buffers in raw sugar color measurement, *J. Sci. Food Agric.*, 75 (1997) 109–116.
- [44] F.A. Adekola, H.I. Adegoke, Adsorption of blue-dye on activated carbons produced from rice husk, coconut shell and coconut coir pith, *Ife J. Sci.*, 7 (2005) 151–157.
- [45] ASTM Standard, Standard Test Method for Total Ash Content of Activated Carbon, Designation D2866-94, 2000.
- [46] P.D. Pathak, S.A. Mandavgane, Preparation and characterization of raw and carbon from banana peel by microwave activation: application in citric acid adsorption, *J. Environ. Chem. Eng.*, 3 (2015) 2435–2447.
- [47] HACH Water Analysis Handbook, 2nd ed., HACH Company, Loveland, CO, 1992.
- [48] B.H. Hameed, D.K. Mahmoud, A.L. Ahmad, Sorption equilibrium and kinetics of basic dye from aqueous solution using banana stalk waste, *J. Hazard. Mater.*, 158 (2008) 499–506.
- [49] M.Y. Noordin, V.C. Venkatesh, S. Sharif, S. Elting, A. Abdullah, Application of response surface methodology in describing the performance of coated carbide tools when turning AISI 1045 steel, *J. Mater. Process. Technol.*, 145 (2004) 46–58.
- [50] L. Alidokht, A.R. Khataee, A. Reyhanitabar, S. Oustan, Cr(VI) Immobilization process in a Cr-spiked soil by zero valent iron nanoparticles: optimization using response surface methodology, *Clean (Weinh)*, 39 (2011) 633–640.
- [51] M.J. Anderson, P.J. Whitcomb, *RSM Simplified: Optimizing Process Using Response Surface Methods for Design Experiments*, Productivity Press, New York, 2005.
- [52] H. Xiao, H. Peng, S. Deng, X. Yang, Y. Zhang, Y. Li, Preparation of activated carbon from edible fungi residue by microwave assisted K_2CO_3 activation—application in reactive black 5 adsorption from aqueous solution, *Bioresour. Technol.*, 111 (2012) 127–133.
- [53] M. Kousha, E. Daneshvar, H. Dopeikar, D. Taghavi, A. Bhatnagar, Box-Behnken design optimization of Acid Black 1 dye biosorption by different brown macroalgae, *Chem. Eng. J.*, 179 (2012) 158–168.
- [54] K.A. Krishnan, K.G. Sreejalekshmi, R.S. Baiju, Nickel (II) adsorption onto biomass based activated carbon obtained from sugarcane bagasse pith, *Bioresour. Technol.*, 102 (2011) 10239–10247.
- [55] Y.J. Yao, F.F. Xu, M. Chen, Z.X. Xu, Z.W. Zhu, Adsorption behaviour of methylene blue on carbon nanotubes, *Bioresour. Technol.*, 101 (2010) 3040–3046.
- [56] I. Langmuir, The adsorption of gases on plane surfaces of glass, mica and platinum, *J. Am. Chem. Soc.*, 40 (1918) 1361–1403.
- [57] H.M.F. Freundlich, Over the adsorption in solution, *J. Phys. Chem.*, 57 (1906) 385–470.
- [58] M.J. Temkin, V. Pyzhev, Recent modifications to Langmuir isotherms, *Acta Phys-Chim. Sin.*, 12 (1940) 217–222.
- [59] P. Gao, Z.H. Liu, G. Xue, B. Han, M.H. Zhou, Preparation and characterization of activated carbon produced from rice straw by $(NH_4)_2HPO_4$ activation, *Bioresour. Technol.*, 102 (2011) 3645–3648.
- [60] C.A. Basar, Applicability of the various adsorption models of three dyes adsorption onto activated carbon prepared waste apricot, *J. Hazard. Mater.*, 135 (2006) 232–241.
- [61] R. Malarvizhi, Y.S. Ho, The influence of pH and the structure of the dye molecules on adsorption isotherm modeling using activated carbon, *Desalination*, 264 (2010) 97–101.
- [62] S. Karagoz, T. Tay, S. Ucar, M. Erdem, Activated carbons from waste biomass by sulfuric acid activation and their use on methylene blue adsorption, *Bioresour. Technol.*, 99 (2008) 6214–6222.
- [63] A.A. Nunes, A.S. Franca, L.S. Oliveira, Activated carbons from waste biomass: an alternative use for biodiesel production solid residues, *Bioresour. Technol.*, 100 (2009) 1786–1792.
- [64] G.O. El-Sayed, M.M. Yehia, A.A. Asaad, Assessment of activated carbon prepared from corncob by chemical activation with phosphoric acid, *Water Resour. Ind.*, 7–8 (2014) 66–75.
- [65] S. Lagergren, About the theory of so called adsorption of soluble substances, *kungl. Svenska Vetenskapsakademien. Handlingar*, Band, 24 (1898) 1–39.
- [66] Y.S. Ho, G. McKay, Pseudo-second order model for sorption processes, *Process Biochem.*, 34 (1999) 451–465.
- [67] W.J. Weber, J.C. Morris, Kinetics of adsorption on carbon from solution, *J. Sanit. Eng. Div.*, 89 (1963) 31–60.